AMERICAN ACADEMY OF OPHTHALMOLOGY®

A Noninvasive Clinical Method to Measure in Vivo Mechanical Strains of the Lamina Cribrosa by OCT

Vanessa Hannay, MS,[1,*] *Cameron Czerpak, PhD,*[1,*] *Harry A. Quigley, MD,*[2] *Thao D. Nguyen, PhD*[1,2]

Objective: To measure mechanical strain of the lamina cribrosa (LC) after intraocular pressure (IOP) change produced 1 week after a change in glaucoma medication.

Design: Cohort study.

Participants: Adult glaucoma patients (23 eyes, 15 patients) prescribed a change in IOP-lowering medication.

Intervention: Noninvasive OCT imaging of the eye.

Main Outcome Measures: Deformation calculated by digital volume correlation of OCT scans of the LC before and after IOP lowering by medication.

Results: Among 23 eyes, 17 eyes of 12 persons had IOP lowering $\geq$ 3 mmHg (reduced IOP group) with tensile anterior-posterior E_{zz} strain = 1.0% $\pm$ 1.1% ($P = 0.003$) and compressive radial strain (E_{rr}) = $-0.3\% \pm 0.5\%$ ($P = 0.012$; random effects models accounting inclusion of both eyes in some persons). Maximum in-plane principal (tensile) strain and maximum shear strain in the reduced-IOP group were as follows: $E_{max} = 1.7\% \pm 1.0\%$ and $\Gamma_{max} = 1.4\% \pm 0.7\%$, respectively (both $P < 0.0001$ vs. zero). Reduced-IOP group strains E_{max} and Γ_{max} were significantly larger with greater % IOP decrease ($P < 0.0001$ and $P < 0.0001$, respectively). The compliances of the E_{zz}, E_{max}, and Γ_{max} strain responses, defined as strain normalized by the IOP decrease, were larger with more abnormal perimetric mean deviation or visual field index values (all $P \leq 0.02$). Strains were unrelated to age (all $P \geq 0.088$). In reduced-IOP eyes, mean LC anterior border posterior movement was only 2.05 μm posteriorly ($P = 0.052$) and not related to % IOP change ($P = 0.94$, random effects models). Only E_{rr} was significantly related to anterior lamina depth change, becoming more negative with greater posterior LC border change ($P = 0.015$).

Conclusions: Lamina cribrosa mechanical strains can be effectively measured by changes in eye drop medication using OCT and are related to degree of visual function loss in glaucoma.

Financial Disclosure(s): Proprietary or commercial disclosure may be found in the Footnotes and Disclosures at the end of this article. *Ophthalmology Science 2024;4:100473*

Supplemental material available at www.ophthalmologyscience.org.

Glaucoma is the second most common cause of blindness worldwide[1] and numerous studies show that lowering intraocular pressure (IOP) slows its progressive vision loss.[2] The level of IOP is a major risk factor for glaucomatous damage, whether IOP is within or above the normal range.[3] Methods to lower IOP include surgery, laser treatment, and eye drop medication. Although modest IOP lowering leads to stable visual function in many glaucoma patients, a minority have a much more aggressive course.[4] At present there are not consistent biomarkers that indicate which eyes will have more rapid progression with standard initial therapy.

Glaucomatous neuropathy results from death of retinal ganglion cells, due in part to injury to their axons at the optic nerve head (ONH) within its lamina cribrosa (LC).[5] The upper and lower zones of the LC, through which the most susceptible axons pass, have been shown to have less dense connective tissue structure and to undergo greater mechanical strain with in vitro inflation testing.[6] This suggests that a clinical measure of LC strain might provide valuable information on which patients and what LC zones would have greater susceptibility to rapid progressive worsening.[7,8] We and others have measured the short-term strain responses of the LC in glaucoma patients after both increases and decreases in IOP, using digital volume correlation of spectral-domain OCT images taken at 2 different IOPs (*OETB*. 2018; 10496:55–61).[9–13] With modest IOP lowering, biomechanical strains are regularly obtainable and fit with the expected deformation of the LC tissue, undergoing expansion in the anterior–posterior direction and contraction in diameter.[14]

https://doi.org/10.1016/j.xops.2024.100473
ISSN 2666-9145/24

Artificial elevation of IOP produced corresponding compression of the lamina. Most importantly, our data and those of Girard et al[11] indicate that eyes with greater loss of retinal ganglion cells have greater LC strain.[14,15] These data suggest that short-term LC strain measurements may provide biomarkers for glaucoma susceptibility.

In the present report, we applied digital volume correlation (DVC) to analyze OCT images of the LC in glaucoma patients before and 1 week after a change of IOP-lowering eye medication to calculate the strains in the LC. Our purpose was to produce a method for clinical strain assessment that would be compatible with standard management approaches in initial glaucoma therapy for any office treating patients that have OCT capability.

Methods

Experimental Subjects

The study was approved by the Johns Hopkins institutional review board and written informed consent was obtained from all subjects, who were patients from the Glaucoma Center of Excellence, Wilmer Ophthalmological Institute, Johns Hopkins Medicine. This study is clinical trial NCT03267849. Data are presented for 23 eyes of 15 patients. Data from additional patients were excluded due to poor image quality. Among the 23 eyes, all but 2 were from patients starting hypotensive eye drops; of those, 1 eye was from a patient instructed to stop eye drops, and the final patient started oral glaucoma medication.

Eyes were imaged by OCT (Spectralis, Heidelberg Engineering) before and 7.3 ± 1.4 days after IOP change, using methods previously described.[14] Before the first imaging session, all eyes underwent a standard glaucoma examination to assess disease progression, which measured their average retinal nerve fiber layer (RNFL) thickness and visual field (VF) status (Zeiss Humphrey Field Analyzer [HFA2i or 3] 24-2 Swedish Interactive Threshold Algorithm [SITA Standard] field tests; Zeiss HFA2i) with the indices mean deviation (MD) and VF index (VFI) within 3 months of imaging. Retinal nerve fiber layer thickness was measured using Cirrus OCT (Zeiss). The mean (± standard deviation) MD for the overall group of 23 eyes was −5.4 decibels (dB) ± 5.7 dB, with 15 eyes having MD > −6 dB, 5 eyes with moderate damage (−12 dB < MD < −6 dB), and 3 eyes with severe damage (MD < −12 dB). The mean thickness of the RNFL ranged from 54 to 83 μm. The age range of the 15 study subjects was 30 to 80 (mean [± standard deviation], 62.1 ± 12.4; median, 64) years.

We divided the 23 eyes into reduced-IOP and unchanged-IOP groups, based on whether or not they underwent significant IOP change. Reduced IOP (n = 17 eyes, 12 patients) was defined as eyes with an IOP decrease ≥ 3 mmHg, while unchanged IOP eyes (6 eyes, 5 patients) had ≤ 1 mmHg change. None of the eyes had IOP change between 1 and 3 mmHg. The 1 patient who stopped eye drops to attempt a change in IOP had no change and is assigned to the unchanged-IOP group. The reduced-IOP group had a higher average baseline IOP (20.3 ± 5.8 mmHg) than the unchanged-IOP group (12.5 ± 5.2 mmHg), but the 2 groups did not differ in the mean age, MD, VFI, or RNFL thickness.

OCT Imaging

Intraocular pressure was measured using a rebound tonometer (iCare Finland Oy) directly before each imaging session. Baseline and posttreatment IOP were each recorded as the mean of 6 consecutive measurements per eye. We previously found that baseline iCare IOP measurements did not differ to those acquired on the same visit using Goldmann applanation tonometry.[14] Of the 23 eyes, 21 eyes were measured with Goldmann applanation at their routine visits. The change in IOP from before to after drops intervention measured by applanation was not significantly different from the change measured by the iCare tonometer (mean difference, 1.0 ± 3.1 mmHg; $P = 0.16$). The IOL Master (Zeiss Meditec) was used to measure the axial lengths and corneal curvatures of each eye. The curvature values were input to Spectralis to calibrate the magnification. The Spectralis was set to high resolution and auto-brightness mode. At each imaging session, 3 consecutive OCT image volumes, consisting of 24 radial scans (ONH-RC scan) equally spaced circumferentially around the ONH, were acquired using enhanced depth imaging mode for each eye. To optimize the image quality of the scans, the visible tissue was centered such that it occupied the lower two-thirds of the window and its brightness was adjusted until it reached the maximum. We refer to the anterior−posterior direction as the Z-direction, the radial direction as the R-direction, and the circumferential direction as the θ-direction. The in-plane resolution of each scan (RZ plane) was 768 × 495 pixels, which translated to 5.17−6.25 μm in R and 3.87 μm in Z. At Bruch's membrane opening, the out-of-plane resolution was approximately 108 μm in θ.

Image Segmentation

Each of the 24 radial scans was segmented by hand using FIJI.[14] Within each OCT scan, the end of Bruch's membrane opening (BMO) was marked on either side of the ONH and the anterior border of the LC was marked where visible between either side of the BMO (Fig 1). The anterior LC markings were fit to a continuous line using piecewise linear interpolation, and a parallel curvilinear border was drawn 250 mm posterior to the anterior border to represent the posterior LC because the actual posterior limit of the LC is typically not visible in OCT images. The LC region was defined as the area between the 2 LC borders and within BMO delineated by vertical lines. Lamina cribrosa thickness of 250 μm is based on our past microscopic measurements of the human LC.[16]

Digital Volume Correlation and Strain Calculations

Before processing with DVC,[17] the speckle pattern in OCT images was enhanced with contrast-limited adaptive histogram equalization in FIJI. A gamma correction of 1.75 was then used to reduce noise in areas of low signal. Images were next imported into MATLAB 2019a (Mathworks) to produce a 3-dimensional matrix of 8-bit intensity values.

We have published in detail the fast iterative DVC method for calculating strains in the human LC,[13,14,18] and an even more detailed description is provided by the original paper Bar-Kochba et al.[17] In short, DVC works by tracking the movement of the natural speckle pattern between 2 sets of images. The algorithm starts by correlating a large subvolume of 256 × 256 × 32 pixels (R, Z, and Q) to calculate the deformation field required to deform the before image to the after image. The algorithm iteratively then refines the subvolume down and calculates the deformation field until it reaches a subvolume of 2 × 2 × 1. These window sizes were chosen to be consistent with Czerpak et al[14] as the large initial subvolumes resolve strains larger than those measured in this study, and the small final subvolume does not change the error calculation because of the iterative nature of the correlations. The quality of the tracking is measured by the correlation coefficient. Values that fall below the threshold of

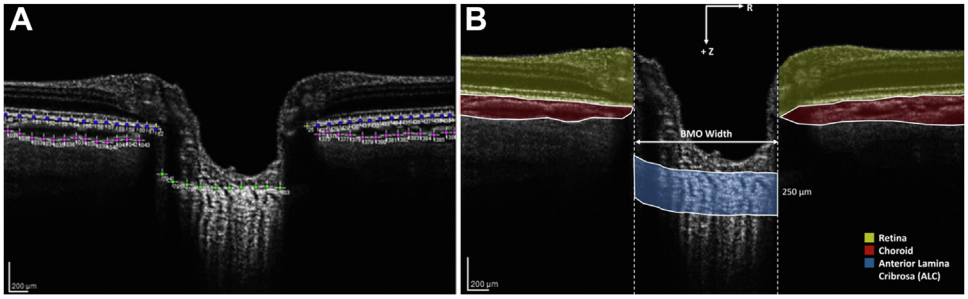

Figure 1. A, Segmentation of slice 1 of the 24 OCT images of the optic nerve head. **B,** The segmented regions including the retina, choroid, BMO, and anterior LC. The anterior LC represents an area of 250 µm below the marked LC surface. BMO = Bruch's membrane opening; LC = lamina cribrosa.

0.055 are removed, meaning that areas of shadows from blood vessels, low image signal, or high noise are not included in strain calculations.

Digital volume correlation was applied to OCT image pairs before and after IOP change to estimate the 3-dimensional displacement field. These were smoothed to calculate the components of the Green−Lagrange strain tensor from the gradient of the displacement field as described in previous work in the LC region.[14] The 3 normal strain components, E_{zz}, E_{rr}, and $E_{\theta\theta}$, indicate local expansions (positive) or contractions (negative) of the tissue in the thickness *(z)*, radial *(r)*, and circumferential (θ) directions. The 3 shear strain components E_{rz}, $E_{r\theta}$, and $E_{\theta z}$, denote local angular distortions in their respective planes. For example, $E_{\theta z}$ for a cylinder results from a twist and $E_{r\theta}$ indicates transformation of the circular cross section into an elliptical cross section. From these strain components, we calculated the maximum principal strain (E_{max}) and maximum shear strain (Γ_{max}) in the RZ plane of the radial OCT images. We also divided strain data into the central and peripheral lamina, using half the radius of the LC outer border as separation. In addition, we divided the LC strain data by quadrant, using an X-shaped delineation to segregate superior, temporal, inferior, and nasal quadrants.

In addition to LC strains, we measured the change in position of the anterior LC border from its displacement (U_z) relative to the position of the BMO. Lamina cribrosa border change was calculated as an average displacement across the entire LC border.

For each eye, we estimated the baseline displacement and strain errors by applying DVC to consecutive OCT image volumes acquired approximately 2 minutes apart of the same ONH at the baseline IOP.[14] Because the consecutive images were acquired under nominally the same IOP, nonzero values of strains and displacements denote error caused by the imaging conditions, image quality, and the imaging correlation algorithm. Digital volume correlation fails or produces high baseline errors in regions of low contrast, such as where the LC is shadowed by overlying blood vessels. These regions excluded from subsequent strain analyses by filtering out points where the correlation coefficient was < 0.055. The resulting average area of accurate DVC correlation was 51.1 ± 21.4% across the 23 image sets. The average baseline displacement error averaged over the LC were 0.016 ± 0.201 mm for U_z, 0.065 ± 0.267 mm for U_r, and 1.43 ± 4.25 mm for U_q. The average baseline strain errors were 0.037 ± 0.118% for E_{zz}, −0.020 ± 0.061% for E_{rr}, −0.019 ± 0.150% for E_{qq}, 0.022 ± 0.102% for E_{rq}, 0.018 ± 0.077% for E_{rz}, and −0.029 ± 0.266% for E_{qz}.

Statistical Analysis

We used paired and unpaired *t* tests, as appropriate, to determine the significance of the mean LC strains compared with no change and to baseline and correlation errors. Relationships between strains and other parameters including age, IOP, LC border movement, and glaucoma damage (MD, VFI, and RNFL thickness) were analyzed using analysis of variance and random effects multivariable regression that account for inclusion of both eyes of some patients. Random effects models accounting effects of inclusion of both eyes for some patients were used in the overall analysis as well as the analysis of the reduced-IOP group. For the unchanged-IOP group, there was only 1 pair of eyes from 1 of the patients, so both eyes were included in the analysis of this group of 6 total eyes without specifically accounting for bilateral inclusion. For all statistical analyses, a P value ≤ 0.05 was considered significant.

Results

IOP and LC Depth Changes

One week after medication change, the reduced-IOP group had a mean ± standard deviation IOP change of −5.8 ± 1.5 mmHg (paired *t* test, $P < 0.001$; 17 eyes of 12 patients), representing a mean decrease from baseline of −29.6% ± 8.2%. The range of IOP change in this group was −3 to −8 mmHg. Mean IOP change in the unchanged IOP group was −0.3 ± 0.8 mmHg ($P = 0.36$, paired *t* test, 6 eyes of 5 patients), or −2.7% ± 8.1%, which was insignificantly below baseline.

The anterior lamina depth (ALD) change from baseline after IOP change was defined as positive if the anterior LC surface moved posteriorly (away from the cornea) and negative if it moved anteriorly (toward the cornea). For reduced-IOP eyes, mean ALD change was 2.05 µm (95% confidence interval, −0.02 to 4.1), random effects model accounting effects of inclusion of both eyes for some patients ($P = 0.052$ compared with zero change). Thus, there was only a small mean posterior movement of the LC, with some eyes moving posteriorly and some anteriorly. Anterior lamina depth change was not significantly related to IOP change nor to percent IOP change ($P = 0.94$, random effects model). In the unchanged-IOP group, mean ALD change was +1.50 ± 2.27 µm, but not significantly different from zero change ($P = 0.17$, paired *t* test).

LC Strains

For the reduced IOP group, the LC strain response to IOP decrease were significantly larger than the baseline

Table 1. Lamina Cribrosa Strains in the Reduced-IOP and Unchanged-IOP Groups

	Reduced IOP	P Value	Unchanged IOP	P Value
E_{zz}	0.010 ± 0.011	**0.003**	0.003 ± 0.003	0.054
E_{rr}	−0.003 ± 0.005	**0.012**	0.001 ± 0.009	0.76
$E_{\theta\theta}$	−0.001 ± 0.009	0.70	−0.002 ± 0.009	0.76
$E_{r\theta}$	0.002 ± 0.008	0.35	−0.011 ± 0.017	0.20
$E_{\theta z}$	−0.001 ± 0.005	0.32	0.001 ± 0.006	0.65
E_{rz}	0.000 ± 0.006	0.77	−0.001 ± 0.004	0.63
E_{max}	0.017 ± 0.010	**< 0.0001**	0.013 ± 0.012	0.053
Γ_{max}	0.014 ± 0.007	**< 0.0001**	0.011 ± 0.009	**0.041**

IOP = intraocular pressure.
Mean strains ± standard deviation (strains are unitless). N = 17 eyes in reduced-IOP group and 6 eyes in unchanged-IOP group.
Bold values indicate statistically significant *P* values.

(reproducibility) error for E_{zz} and E_{rr} strains ($P = 0.002$, 0.011, respectively, random effects models) (Table 1, Figs 2, 3; Fig S4, available at www.ophthalmologyscience.org). The normal strain in the thickness direction $E_{zz} = 1.0\% \pm 1.1\%$ was tensile (> 0, $P = 0.003$) and the radial strain E_{rr} was compressive ($-0.3\% \pm 0.5\%$; $P = 0.012$). In addition, the maximum principal (tensile) strain and maximum shear strain in the reduced-IOP group were significantly > 0: $E_{max} = 1.7\% \pm 1.0\%$ and $\Gamma_{max} = 1.4\% \pm 0.7\%$; (both $P < 0.0001$). The analysis for the full group is included in the supplement (Tables S2–S10, available at www.ophthalmologyscience.org). The results were generally the same as for the IOP-change group. Some comparisons were less significant because 25% of the outcomes had no IOP change.

For the unchanged-IOP group, which served here as a form of control group, strains had only borderline significant differences from zero in E_{zz}, E_{max}, and Γ_{max} ($P = 0.054$, 0.053, 0.041, respectively). The mean E_{zz} for this group was $0.3\% \pm 0.3\%$, 3 times smaller than that of the reduced-IOP eyes and not significantly greater than baseline error ($P = 0.08$).

There were no significant differences in either group in E_{zz} or E_{max} strains in the central compared with the peripheral LC (all $P > 0.63$ for reduced-IOP group; all $P > 0.34$ for unchanged-IOP group), nor did strains differ significantly by LC quadrant (all $P > 0.65$ for reduced-IOP group; all $P > 0.66$ for unchanged-IOP group).

LC Strains in Reduced-IOP Group Compared with Other Variables

In the reduced-IOP group, strains E_{max} and Γ_{max} were significantly larger with greater % IOP decrease, whereas E_{rr} was significantly more negative with greater % IOP decrease (for % decrease: < 0.0001, < 0.0001, and $P = 0.048$, respectively, random effects models; Fig 5). E_{max} and Γ_{max} strains were also significantly associated with the magnitude of IOP decrease ($P = 0.0029$, 0.0020, respectively, random effects models). All strains were unrelated to patient age (all $P \geq 0.088$). Axial length was measured in 18 eyes before drops intervention and was

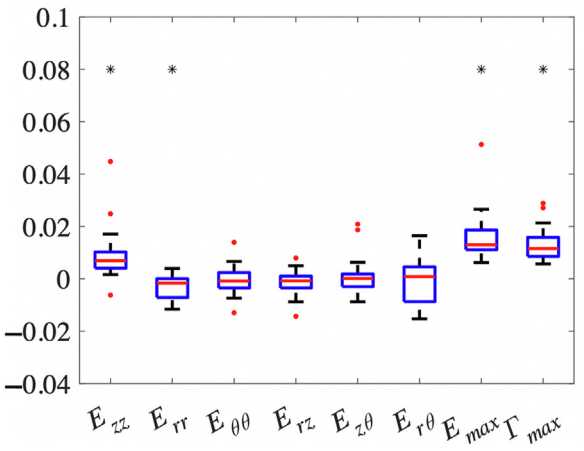

Figure 2. Strains in reduced intraocular pressure group (n = 17 eyes) where asterisk (*) indicates *P* value ≤ 0.05.

not related to strain (all $P > 0.07$). Among all strains, only E_{rr} was significantly related to ALD change, becoming more negative with greater posterior ALD change ($P = 0.015$). Strain data were compared with the degree of glaucoma damage in VF and RNFL thickness. Strains were not significantly related to either MD or VFI indexes in field data (all $P \geq 0.14$). Strains E_{zz}, E_{max}, and Γ_{max} were larger as RNFL thickness increased in models (all $P < 0.001$). This outcome appeared to be due to 2 outlying values with higher RNFL thickness (Fig S6, available at www.ophthalmologyscience.org).

Because we determined that strains were related to the degree of IOP lowering, we calculated for each strain response the value called compliance, defined as the strain per mmHg IOP decrease. In random effects models, compliances of strains E_{zz}, E_{max}, and Γ_{max} were significantly larger with more abnormal MD index values in the VF ($P = 0.02$, 0.001, and 0.011, respectively, Fig 7). Likewise, compliances for E_{max} and Γ_{max} were larger with worsening VFI ($P = 0.015$ and 0.010, respectively). Compliances for the same 3 strains (E_{zz}, E_{max}, and Γ_{max}) were significantly related to RNFL thickness, but when the 2 outlying values were omitted from the analysis there was no demonstrable relation of strains to RNFL thickness.

Discussion

These data confirm our previous findings that reduction of IOP leads to measurable strains in the LC with sequential OCT imaging. There are several similarities to our initial reports. In Czerpak et al,[14] we imaged eyes before and 20 minutes after postoperative laser suturelysis in eyes that had undergone trabeculectomy. The patients in that report had somewhat greater structural and functional damage (mean MD, -11.5 ± 8.9 dB) than the eyes in this data set (for reduced IOP group: mean MD, -6.6 ± 5.8 dB), and the suturelysis eyes had greater mean IOP lowering. Despite these differences, the strains measured 1 week after changes in eye medication were similar to those

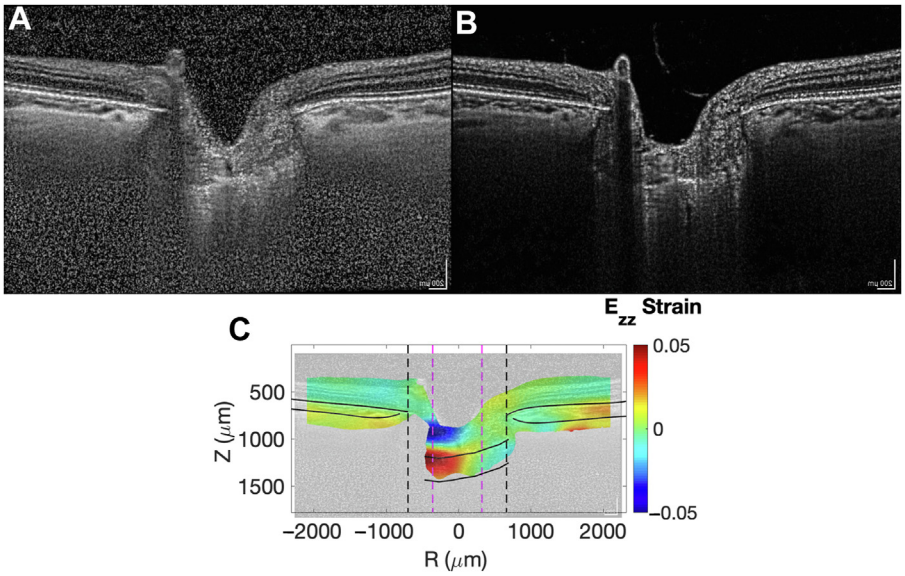

Figure 3. OCT images following CLAHE and gamma filtering, and the E_{zz} strain map for a person who struggled with imaging. **A,** Before OCT image. **B,** After intraocular pressure change OCT image. **C,** The E_{zz} strain map where dark red regions indicate local expansion in the anterior-posterior direction, and dark blue regions indicate local contraction. OCT images with high signal-to-noise ratio can be found in Figure S4. CLAHE = contrast-limited adaptive histogram equalization.

immediately after suturelysis. This suggests that after IOP lowering, the LC exhibits a time-dependent behavior with strain increasing more at 1 week than after 20 minutes. The time dependence can be caused by tissue viscoelasticity and remodeling of the tissue structure. It is unlikely that the collagen structure will be remodeled after 1 week of IOP lowering, but other tissue structures can be remodeled quickly. The short-term remodeling repones of the ONH over 1 week may also influence the strains measured in this study. One group found that experimental IOP increase by 2 minutes of ophthalmodynamometry pressure on the eye has also demonstrated measurable strains, but with dramatically greater IOP elevations.[9] Our findings show that a simple change in eye drop medication produces strains in the LC that are assessable at a typical follow-up visit. There may be an advantage to methods of IOP lowering for which strain can be measured after $\geq$ 1 week to produce more easily measurable strain values.

Furthermore, these data provide further evidence that eyes with greater VF damage have greater, not less, LC strain. We[14] and others[15] have previously found that eyes exhibiting worse injury have a more compliant LC. In fact, we also found similarly, in study of control and glaucoma eyes post mortem, that eyes with worse histological axon loss had greater compliance than mildly damaged eyes.[19,20] These findings seem to contradict prior conclusions that all tissues of the optic nerve in glaucoma eyes are stiffer after suffering damage like the stiffening found in the sclera with glaucoma. Prior research, however, did not routinely measure LC strains, but rather employed indirect measures of portions of the sclera more distant from the peripapillary area.[21,22] We previously measured the LC strain in ex vivo inflation tests and found that the LC strain response of mildly damaged glaucoma eyes was stiffer than those of undamaged normal eyes.[20] The most relevant zones for glaucoma

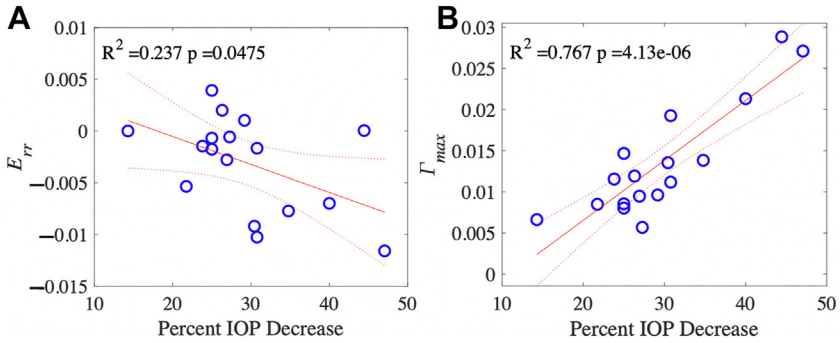

Figure 5. A higher percent decrease in IOP was associated with (**A**) more radial contraction (negative E_{rr}) and (**B**) larger maximum shear strain (Γ_{max}). Data from reduced-IOP group (n = 17 eyes). Linear regression analysis. IOP = intraocular pressure.

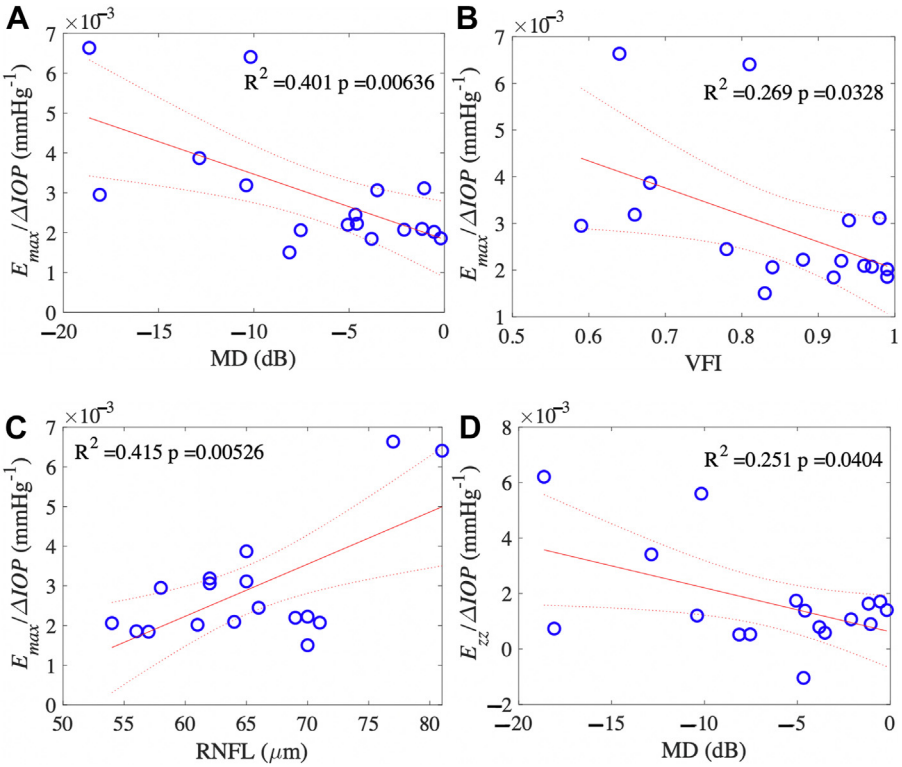

Figure 7. Eyes with greater glaucoma progression as indicated by (**A**) more negative MD and (**B**) lower VFI had greater compliance of maximum principal strain (E_{max}/ΔIOP), indicating a softer strain response. **C,** However, a thicker RNFL thickness was associated with greater compliance of E_{max}. **D,** A more negative MD was associated with greater compliance of E_{zz}. Data from reduced-IOP group (n = 17 eyes). Linear regression analysis.ΔIOP = change in intraocular pressure; MD = mean deviation; RNFL = retinal nerve fiber layer; VFI = visual field index.

damage are in the immediate ONH region. Conceivably, the greater strains we have estimated in the LC with worse damage could result from greater glaucoma damage, causing remodeling in which LC beams become thinner.[23] Indeed, LC curvature in inflation testing was greater with greater damage, implying a more compliant response (*Invest Ophthalmol Vis Sci.* 2021;62:1656). Both monkeys with chronic IOP elevation and human glaucoma eyes are reported to have a thinner-than-normal LC, suggesting more compliant, not stiffer, behavior.[24,25] The peripapillary sclera in experimental and human glaucoma has a less ordered circumferential fiber pattern[26,27] that may behave more rigidly, intensifying the effect of the translaminar pressure gradient to cause greater LC strain. Indeed, we have estimated posterior scleral strains using the OCT method described here, and find that scleral strains are proportionately smaller than the LC of the same eye, and that the strains in the 2 zones are significantly related to each other.[28] We must keep in mind that our data are cross sectional and do not indicate what the strain state of damaged glaucoma eyes was at baseline.

The medication change approach produced not only similar magnitudes of strains, but strain change in the same directions as our previous data after suturelysis. Intraocular pressure decrease in both paradigms caused the LC to expand in thickness (E_{zz} strain) and to contract in radius (E_{rr} strain). One could visualize this change as if the LC were a container that changed shape from a tuna fish can to an orange juice can. In both studies, larger IOP decreases led to more tensile E_{zz} and greater maximum principal (E_{max}) and maximum shear strains (Γ_{max}). Likewise, there were consistent findings that greater compliance of E_{max} and Γ_{max} were associated with worse MD and VFIs. In both situations, the ALD change was minimal in this time frame.

Interestingly, the single difference with our previous study was the fact that greater strain was associated with thicker average RNFL in this study, but thinner RNFL in our suturelysis data. However, this result deserves further study with greater numbers of eyes, as it seems to have been generated largely by 2 outlying values. It is well-known that RNFL thickness more rapidly declines than VF sensitivity in glaucoma. In our previous study, the vast majority of eyes had RNFL average thickness values < 65 μm, while in the present study, the majority had RNFL thickness > 65 μm. By contrast, the VFIs are a more continuous reflection of glaucoma damage, whereas the RNFL data decline earlier and have a floor effect at 50 μm. The seeming difference in our 2 studies related to structural glaucoma damage related to strains may actually, therefore, be another indication that stage of glaucoma damage is related to LC strain behavior.

The validity of these OCT strain measurements was further confirmed by the finding that strains exceeded the reproducibility error. Furthermore, in dividing our test subjects into those whose IOP did not change with medication alteration and those that did, we could show that

strains were largely insignificant when IOP was not different from baseline.

The main outcome of our study is LC strain and does not depend on the position or change in position of the BMO. However, the LC depth change is the displacement of the LC anterior surface relative to BMO. Lamina cribrosa depth data dependence on the reference plane is a less definitive method for determining the deformation and biomechanical behavior of the LC. Our calculation of displacement of the anterior lamina surface is the difference in ALD at the 2 pressures averaged over the surface. This takes into account the motion of the BMO with pressure change to minimize its influence.

Although our data had significant associations with the present sample, it will be important to substantially expand the data set to confirm several important hypotheses. Further studies should include imaging of nonglaucoma control persons who would consent to take eyedrops to lower IOP. These should include both fully normal, age-matched persons, as well as ocular hypertensive eyes with no damage. The expansion of the sample size could also allow estimation of the potential effects on strain of other variables, such as age, axial length, refraction, sex, and race. Our statistical method accounted for the inclusion of both eyes of some patients, but further work should expand the bilateral testing to explore the possibility that an eye that is more damaged, or more likely to be damaged in the future, has different strain behavior.

In conclusion, the use of DVC analysis of OCT images before and after IOP change is a feasible means for measuring in vivo LC strains. The strain measures were confirmed as greater with worse VF damage, suggesting that with further research such imaging may provide a biomarker for glaucoma susceptibility at routine clinic visits. Longitudinal studies are merited to investigate the biomechanical response to IOP change over time in these patients.

Footnotes and Disclosures

Originally received: October 11, 2023.
Final revision: January 4, 2024.
Accepted: January 12, 2024.
Available online: January 20, 2024.Manuscript no. XOPS-D-23-00216R2.

[1] Department of Mechanical Engineering, The Johns Hopkins University, Baltimore, Maryland.

[2] Department of Ophthalmology, Wilmer Ophthalmological Institute, Johns Hopkins University School of Medicine, Baltimore, Maryland.

*V.H. and C.C. contributed equally to this work.

Disclosures:

All authors have completed and submitted the ICMJE disclosures form.

The author(s) have made the following disclosure(s):

H.A.Q.: Receipt of equipment − Heidelberg Engineering.

The other authors have no proprietary or commercial interest in any materials discussed in this article.

This research was funded in part by NIH NEI R01 EY02120 (H.A.Q.), P30 EY01765 (Wilmer Institute Core Grant), Research to Prevent Blindness, and the A. Edward Maumenee Professorship (H.A.Q.) and Brightfocus G2021012S (T.D.N.).

HUMAN SUBJECTS: Human subjects were included in this study. The study was approved by the Johns Hopkins institutional review board and written informed consent was obtained from all subjects, who were patients from Glaucoma Center of Excellence, Wilmer Ophthalmological Institute, Johns Hopkins Medicine. All research adhered to the tenets of the Declaration of Helsinki.

No animal subjects were used in this study.

Author Contributions:

Conception and design: Quigley, Nguyen

Data collection: Hannay, Czerpak

Analysis and interpretation: Hannay, Czerpak, Quigley, Nguyen

Obtained funding: Quigley, Nguyen

Overall responsibility: Hannay, Czerpak, Quigley, Nguyen

Abbreviations and Acronyms:
ALD = anterior lamina depth; **BMO** = Bruch's membrane opening; **dB** = decibels; **DVC** = digital volume correlation; **IOP** = intraocular pressure; **LC** = lamina cribrosa; **MD** = mean deviation; **ONH** = optic nerve head; **RNFL** = retinal nerve fiber layer; **VF** = visual field; **VFI** = visual field index.

Keywords:
Glaucoma, Lamina cribrosa, Optic nerve head, Digital volume correlation, Optical coherence tomography.

Correspondence:
Harry A. Quigley, MD, 900 Bellemore Road, Baltimore, MA 21210. E-mail: hquigley@jhmi.edu.

References

1. Tham YC, Li X, Wong TY, et al. Global prevalence of glaucoma and projections of glaucoma burden through 2040: a systematic review and meta-analysis. *Ophthalmology*. 2014;121:2081−2090.
2. Heijl A, Leske MC, Bengtsson B, et al. Reduction of intraocular pressure and glaucoma progression: results from the Early Manifest Glaucoma Trial. *Arch Ophthalmol*. 2002;120:1268−1279.
3. Boland MV, Quigley HA. Risk factors and open-angle glaucoma: classification and application. *J Glaucoma*. 2007;16:406−418.
4. Chauhan BC, Malik R, Shuba LM, et al. Rates of glaucomatous visual field change in a large clinical population. *Invest Ophthalmol Vis Sci*. 2014;55:4135−4143.
5. Quigley HA, Addicks EM, Green WR, Maumenee AE. Optic nerve damage in human glaucoma. II. The site of injury and susceptibility to damage. *Arch Ophthalmol*. 1981;99:635−649.
6. Quigley HA, Addicks EM. Regional differences in the structure of the lamina cribrosa and their relation to glaucomatous optic nerve damage. *Arch Ophthalmol*. 1981;99:137−143.
7. Burgoyne CF, Downs JC, Bellezza AJ, et al. The optic nerve head as a biomechanical structure: a new paradigm for understanding the role of IOP-related stress and strain in the pathophysiology of glaucomatous optic nerve head damage. *Prog Retin Eye Res*. 2005;24:39−73.

8. Quigley HA. The contribution of the sclera and lamina cribrosa to the pathogenesis of glaucoma: diagnostic and treatment implications. *Prog Brain Res*. 2015;220:59–86.
9. Beotra MR, Wang X, Tun TA, et al. In vivo three-dimensional lamina cribrosa strains in healthy, ocular hypertensive, and glaucoma eyes following acute intraocular pressure elevation. *Invest Ophthalmol Vis Sci*. 2018;59:260–272.
10. Zhang L, Beotra MR, Baskaran M, et al. In vivo measurements of prelamina and lamina cribrosa biomechanical properties in humans. *Invest Ophthalmol Vis Sci*. 2020;61:27. https://doi.org/10.1167/iovs.61.3.27.
11. Girard MJA, Beotra MR, Chin KS, et al. In vivo 3-dimensional strain mapping of the optic nerve head following intraocular pressure lowering by trabeculectomy. *Ophthalmology*. 2016;123:1190–1200.
12. Wang X, Beotra MR, Tun TA, et al. In vivo 3-dimensional strain mapping confirms large optic nerve head deformations following horizontal eye movements. *Invest Ophthalmol Vis Sci*. 2016;57:5825–5833.
13. Midgett DE, Quigley HA, Nguyen TD. In vivo characterization of the deformation of the human optic nerve head using optical coherence tomography and digital volume correlation. *Acta Biomater*. 2019;96:385–399.
14. Czerpak CA, Kashaf MS, Zimmerman BK, et al. The strain response to intraocular pressure decrease in the lamina cribrosa of patients with glaucoma. *Ophthalmol Glaucoma*. 2022;6:11–22.
15. Chuangsuwanich T, Tun TA, Braeu FA, et al. Differing associations between optic nerve head strains and visual field loss in patients with normal- and high-tension glaucoma. *Ophthalmology*. 2023;130:99–110.
16. Quigley HA, Hohman RM, Addicks EM, et al. Morphologic changes in the lamina cribrosa correlated with neural loss in open-angle glaucoma. *Am J Ophthalmol*. 1983;95:673–691.
17. Bar-Kochba E, Toyjanova J, Andrews E, et al. A fast iterative digital volume correlation algorithm for large deformations. *Exp Mech*. 2015;55:261–274.
18. Midgett DE, Pease ME, Jefferys JL, et al. The pressure-induced deformation response of the human lamina cribrosa: analysis of regional variations. *Acta Biomater*. 2017;53:123–139.
19. Midgett DE, Jefferys JL, Quigley HA, Nguyen TD. The inflation response of the human lamina cribrosa and sclera: analysis of deformation and interaction. *Acta Biomater*. 2020;106:225–241.
20. Midgett D, Liu B, Ling YTT, et al. The effects of glaucoma on the pressure-induced strain response of the human lamina cribrosa. *Invest Ophthalmol Vis Sci*. 2020;61:41. https://doi.org/10.1167/iovs.61.4.41.
21. Coudrillier B, Tian J, Alexander S, et al. Biomechanics of the human posterior sclera: age- and glaucoma-related changes measured using inflation testing. *Invest Ophthalmol Vis Sci*. 2012;53:1714–1728.
22. Grytz R, Fazio MA, Girard MJ, et al. Material properties of the posterior human sclera. *J Mech Behav Biomed Mater*. 2014;29:602–617.
23. Guan C, Pease ME, Quillen S, et al. Quantitative microstructural analysis of cellular and tissue remodeling in human glaucoma optic nerve head. *Invest Ophthalmol Vis Sci*. 2022;63:18.
24. Yang H, Ren R, Lockwood H, et al. The connective tissue components of optic nerve head cupping in monkey experimental glaucoma part 1: global change. *Invest Ophthalmol Vis Sci*. 2015;56:7661–7678.
25. Jonas JB, Berenshtein E, Holbach L. Anatomic relationship between lamina cribrosa, intraocular space, and cerebrospinal fluid space. *Invest Ophthalmol Vis Sci*. 2003;44:5189–5195.
26. Pijanka JK, Coudrillier B, Ziegler K, et al. Quantitative mapping of collagen fiber orientation in non-glaucoma and glaucoma posterior human sclerae. *Invest Ophthalmol Vis Sci*. 2012;53:5258–5270.
27. Boote C, Sigal IA, Grytz R, et al. Scleral structure and biomechanics. *Prog Retin Eye Res*. 2020;74:100773. https://doi.org/10.1016/j.preteyeres.2019.100773.
28. Yuan Z, Czerpak CA, Kashaf MS, et al. Biomechanical strain responses in the optic nerve head region in glaucoma patients after intraocular pressure lowering. *medRxiv*. Posted online June 1, 2023. https://doi.org/10.1101/2023.05.30.23290662.